Security Classification

DOCUMENT CONTROL DATA - R & D

(Security classification of title, body of abstract and indexing annotation must be entered when the overall report is classified)

1. ORIGINATING ACTIVITY *(Corporate author)* Naval Research Laboratory Washington, D.C. 20390	2a. REPORT SECURITY CLASSIFICATION Unclassified 2b. GROUP

3. REPORT TITLE

A REASSESSMENT OF FRACTURE-SAFE OPERATING CRITERIA FOR REACTOR VESSEL STEELS BASED ON CHARPY-V PERFORMANCE

4. DESCRIPTIVE NOTES *(Type of report and inclusive dates)*

This is a special interpretative report.

5. AUTHOR(S) *(First name, middle initial, last name)*

F. J. Loss, J. R. Hawthorne, and C. Z. Serpan, Jr.

6. REPORT DATE September 8, 1970	7a. TOTAL NO. OF PAGES 28	7b. NO. OF REFS 21
8a. CONTRACT OR GRANT NO. NRL Problem M01-14 b. PROJECT NO. Projects RR 007-11-41-5409 and c. AEC-AT(49-5)-2110 d.	9a. ORIGINATOR'S REPORT NUMBER(S) NRL Report 7152 9b. OTHER REPORT NO(S) *(Any other numbers that may be assigned this report)*	

10. DISTRIBUTION STATEMENT

This document has been approved for public release and sale; its distribution is unlimited.

11. SUPPLEMENTARY NOTES Sponsored by U.S. Atomic Energy Commission	12. SPONSORING MILITARY ACTIVITY Department of the Navy (Office of Naval Research), Arlington, Va. 22217

13. ABSTRACT

Fracture-safe operating criteria for commercial nuclear pressure vessels based on Fracture Analysis Diagram procedures and Charpy-V energy trends are reappraised with respect to the effects of thick-section mechanical constraint and low Charpy-V shelf energies resulting from neutron irradiation. Comparisons of the Charpy-V test with the more definitive Dynamic Tear test procedures indicate the former to be an acceptable means of assessing the fracture toughness of A533-B steel. The mechanical constraint associated with 12-in. thicknesses of this steel suggests the addition of 70°F (39°C) to the existing criterion requiring vessel operation above NDT + 60°F (33°C). Ratio Analysis Diagram procedures are shown to be useful in interpreting Charpy-V shelf level data obtained from vessel surveillance programs in terms of critical toughness levels relating to brittle fracture.

DD FORM 1 NOV 65 1473 (PAGE 1)

S/N 0101-807-6801

Security Classification

Security Classification

14. KEY WORDS	LINK A ROLE	LINK A WT	LINK B ROLE	LINK B WT	LINK C ROLE	LINK C WT
Fracture-safe design						
Thick-section steels						
Nuclear pressure vessels						
Fracture toughness tests						
A533-B steel						
Fracture mechanics tests						
Size effect						
Impact tests						
Irradiation-induced toughness degradation						
Charpy-V notch test						
Dynamic tear test						

DD FORM 1 NOV 65 1473 (BACK)

(PAGE 2)

Security Classification

CONTENTS

Abstract	ii
Problem Status	ii
Authorization	ii
INTRODUCTION	1
DYNAMIC TEAR TEST DESCRIPTION	2
CHARPY-V AND DYNAMIC TEAR TRANSITION TEMPERATURE COMPARISONS	5
TRANSITION TEMPERATURE CHARACTERISTICS OF THICK-SECTION A533-B STEEL	9
SHELF LEVEL ANALYSIS	15
Thin Sections	15
Thick Sections	20
SUMMARY	21
REFERENCES	23

ABSTRACT

Fracture-safe operating criteria for commercial nuclear pressure vessels based on Fracture Analysis Diagram procedures and Charpy-V energy trends are reappraised with respect to the effects of thick-section mechanical constraint and low Charpy-V shelf energies resulting from neutron irradiation. Comparisons of the Charpy-V test with the more definitive Dynamic Tear test procedures indicate the former to be an acceptable means of assessing the fracture toughness of A533-B steel. The mechanical constraint associated with 12-in. thicknesses of this steel suggests the addition of 70°F (39°C) to the existing criterion requiring vessel operation above NDT + 60°F (33°C). Ratio Analysis Diagram procedures are shown to be useful in interpreting Charpy-V shelf level data obtained from vessel surveillance programs in terms of critical toughness levels relating to brittle fracture.

PROBLEM STATUS

This is a special interpretative report on fracture-safe design covering various areas of the problem. The major portion of the studies is continuing under the established problem.

AUTHORIZATION

NRL Problem M01-14
Projects RR 007-11-41-5409 and AEC-AT(49-5)-2110

Manuscript submitted July 6, 1970.

A REASSESSMENT OF FRACTURE-SAFE OPERATING CRITERIA FOR REACTOR VESSEL STEELS BASED ON CHARPY-V PERFORMANCE

INTRODUCTION

Nuclear pressure vessels may contain undetected or fatigue-extended flaws. These flaws could result in brittle fracture if a vessel is not operated subject to limitations based on the temperature-induced toughness transition from brittle to ductile behavior or if the high toughness associated with the ductile regime is sufficiently degraded through irradiation. It is desirable to operate these vessels in accordance with criteria chosen to prevent unstable fracture resulting from a large flaw of "reasonable" proportions even for stresses approaching yield levels. To assure such a condition, commercial* water-cooled pressure vessels are generally operated only at temperatures in excess of 60°F (33°C) above the Nil Ductility Transition (NDT) temperature.

The NDT temperature is determined from the Drop Weight Test (DWT) (1) and constitutes a primary index temperature for the Fracture Analysis Diagram (FAD) interpretative approach to brittle fracture prevention on which the "NDT + 60" criterion is based (2). The FAD applies to carbon and low-alloy steels in relatively thin sections† which exhibit a sharp transition from brittle to ductile behavior within a limited temperature increment above NDT. At temperatures above NDT + 60°F, it has been demonstrated from the FAD that flaws several feet in length still require stresses in excess of yield to propagate.

Reactor vessels often contain surveillance specimens which are tested periodically over the vessel lifetime to assess the progressive changes in toughness with neutron exposure. The space available for these specimens generally prohibits the use of the drop weight specimen. The Charpy-V (C_v) specimen, because of its wide use and small size, has been adopted as a primary specimen for surveillance and accelerated exposure studies. A C_v correlation energy or "fix" is normally determined for a particular steel to index the NDT temperature. The radiation-induced toughness degradation is assessed by shifts to higher temperatures in the NDT as determined by this fix energy. Early NRL investigations (3) validated this procedure by showing excellent correlation for several low-alloy structural steels between the increase in the C_v 30-ft-lb temperature, selected as an arbitrary NDT index, and the measured increase in the NDT temperature. Special procedures for reactor operation are called for when the vessel NDT + 60°F limit approaches the startup or shutdown temperature regions of the system.

A reevaluation of existing fracture-safe operating criteria has been necessitated because of (a) the trend toward increasing vessel wall thicknesses whereby mechanical constraint can extend to higher temperatures the plane strain regime near the NDT temperature which is analyzable with linear elastic fracture mechanics (LEFM) methods, thereby questioning the expected temperature transition to high ductility, and (b) an increased awareness of the fact that brittle fracture of thin sections can still take place at NDT + 60°F, if the C_v upper shelf energy level has been substantially reduced by irradiation or is low to begin with. It has been suggested that revised fracture prevention criteria be based on fracture test procedures that are more definitive than the C_v test. This is a

*References to reactors relate to commercial nuclear power plants for the production of electricity.

†Thin section is considered in this report to be less than 3-in. thick.

valid point since cases can be cited for steels (though not usually for the A533-B steel used for the majority of commercial nuclear pressure vessels) where the C_v does not properly define the transition temperature region and does not adequately discriminate between changes in shelf level toughness (4). However, the commercial reactor surveillance data which will be available for many years to come will consist primarily of data from C_v specimens. Therefore, a critical assessment must be made of the value of these data with respect to future safe operation of commercial power reactors and of the existence of additional correlations with other more definitive methods which may be used to enhance the C_v results.

This report reappraises the current fracture-safe operating criteria based on the C_v test for A302-B and A533-B pressure vessel steels in terms of the newer Dynamic Tear (DT) test procedures developed by NRL. Correlations are presented between the C_v and DT tests for unirradiated and irradiated A533-B steels considering both transition temperature and shelf level temperature regimes. The critical flaw size-stress level associated with a particular C_v shelf value for thin sections is evaluated in terms of the Ratio Analysis Diagram (RAD). Areas of uncertainty with respect to C_v shelf toughness for thick sections are reviewed. Implications relating to the effects of thick-section mechanical constraint in the transition temperature region are discussed in terms of thick-section DT and fracture mechanics investigations.

DYNAMIC TEAR TEST DESCRIPTION

The DT test procedure defines a limiting transition temperature region by imposing on a material the maximum severity mechanical conditions which could occur in service. These conditions are dynamic loading, sufficient "crack run" to develop the characteristics of a propagating fracture, a defined thickness constraint, and a deep, sharply notched crack starter region usually formed by an embrittled electron beam weld through the specimen thickness. Other less severe mechanical conditions can define a nonconservative transition region at lower temperatures. The DT test procedure is not designed solely for the transition temperature materials to which this report is addressed, but it is a broad spectrum test capable of also indexing the fracture toughness of ultrahigh-strength steels and aluminum and titanium alloys which exhibit little change in toughness over a wide temperature interval.

Various size DT specimens are used and range in thickness from 5/8 in. to 12 in. The larger sizes simulate the mechanical constraint and variable toughness (metallurgical) through the thickness of heavy-section materials (5). The DT specimen overcomes the disadvantages of the C_v specimen with respect to the relatively dull notch of the latter and lack of sufficient crack run for tough materials. For example, to the authors' knowledge the C_v test never displays a full-slant fibrous fracture when this failure mode is exhibited by a structure. In certain cases the C_v test can give accurate indications of fracture toughness trends for a given material. This fact can most easily be established through correlations with the DT test.

The DT specimen consists of a three-point-loaded beam that is impacted by a falling weight or swinging pendulum (Fig. 1), and the energy to fracture the specimen is recorded. The 5/8-in. specimen shown in Fig. 1 illustrates the alternate method of notch preparation for this specimen consisting of a deep, machined slit with a knife-sharpened tip. The test procedures for both the 5/8-in. and 1-in. DT specimens have been standardized (6,7). The 5/8-in. specimen has been irradiated, and its performance relative to the C_v specimen is discussed in the following sections.

A typical 5/8-in. DT curve for transition temperature materials is shown in Fig. 2 for an A533-B steel of high shelf toughness. The NDT temperature consistently indexes

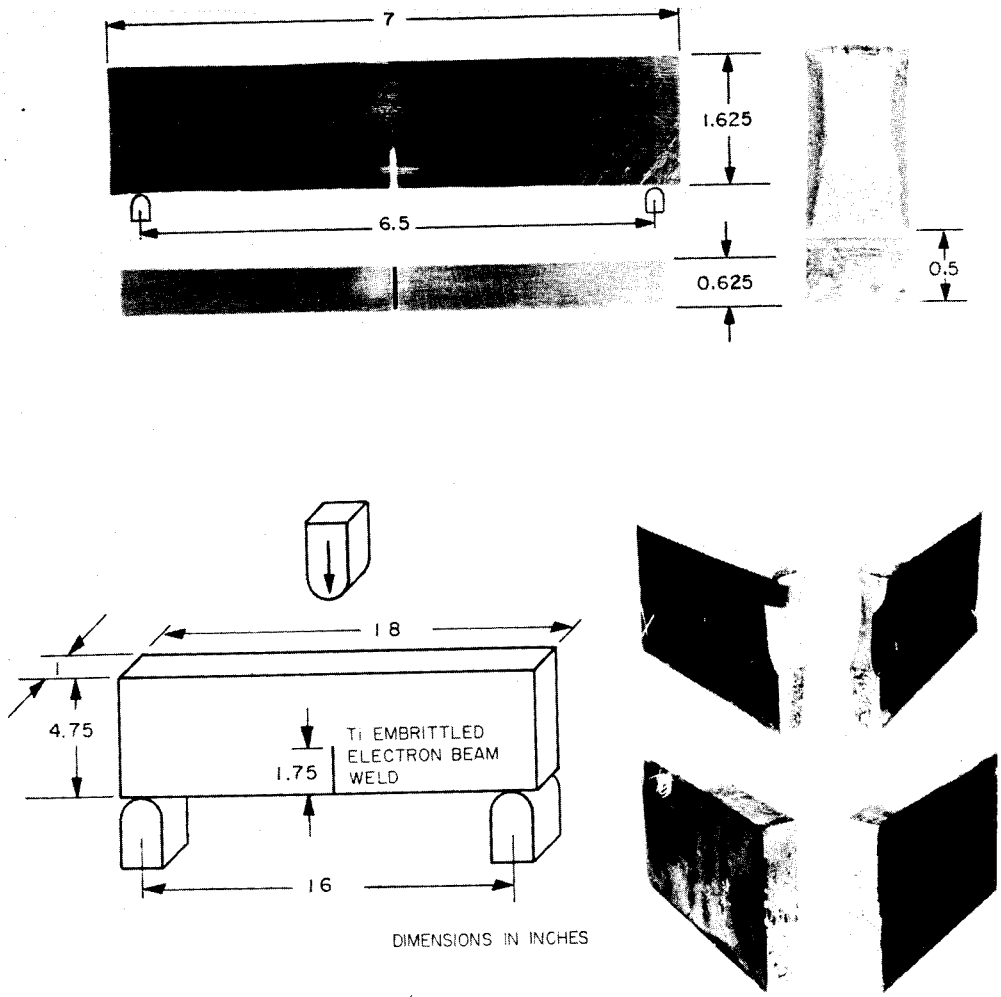

Fig. 1 - Features of 5/8-in. and 1-in. DT specimens. The 5/8-in. specimen (top) is illustrated with a machined slit crack starter having a knife-edge-sharpened notch tip. The 1-in. specimen (bottom) contains a brittle electron beam weld crack starter, which is also used for the 5/8-in. DT specimen. The broken halves of the 1-in. DT specimens illustrate ductile- and brittle-type fractures.

the DT toe region or beginning of the sharp transition temperature increase in fracture energy.* The temperatures of this toe region define a region of brittle behavior that is analyzable with dynamic LEFM techniques. It has been shown that the NDT temperature is equivalent to a ratio of the dynamic plane strain fracture toughness K_{Id} to the dynamic yield stress σ_{yd}, of approximately 0.5 (5). The toughness increases sharply within a relatively small temperature interval above the NDT temperature to a level requiring gross plastic deformation to propagate flaws near the shelf temperatures, provided the shelf is of a high level.

*The mechanical constraint associated with thick sections, however, can extend the initial portion of the region of sharp energy increase which evolves at temperatures above the NDT temperature as discussed later.

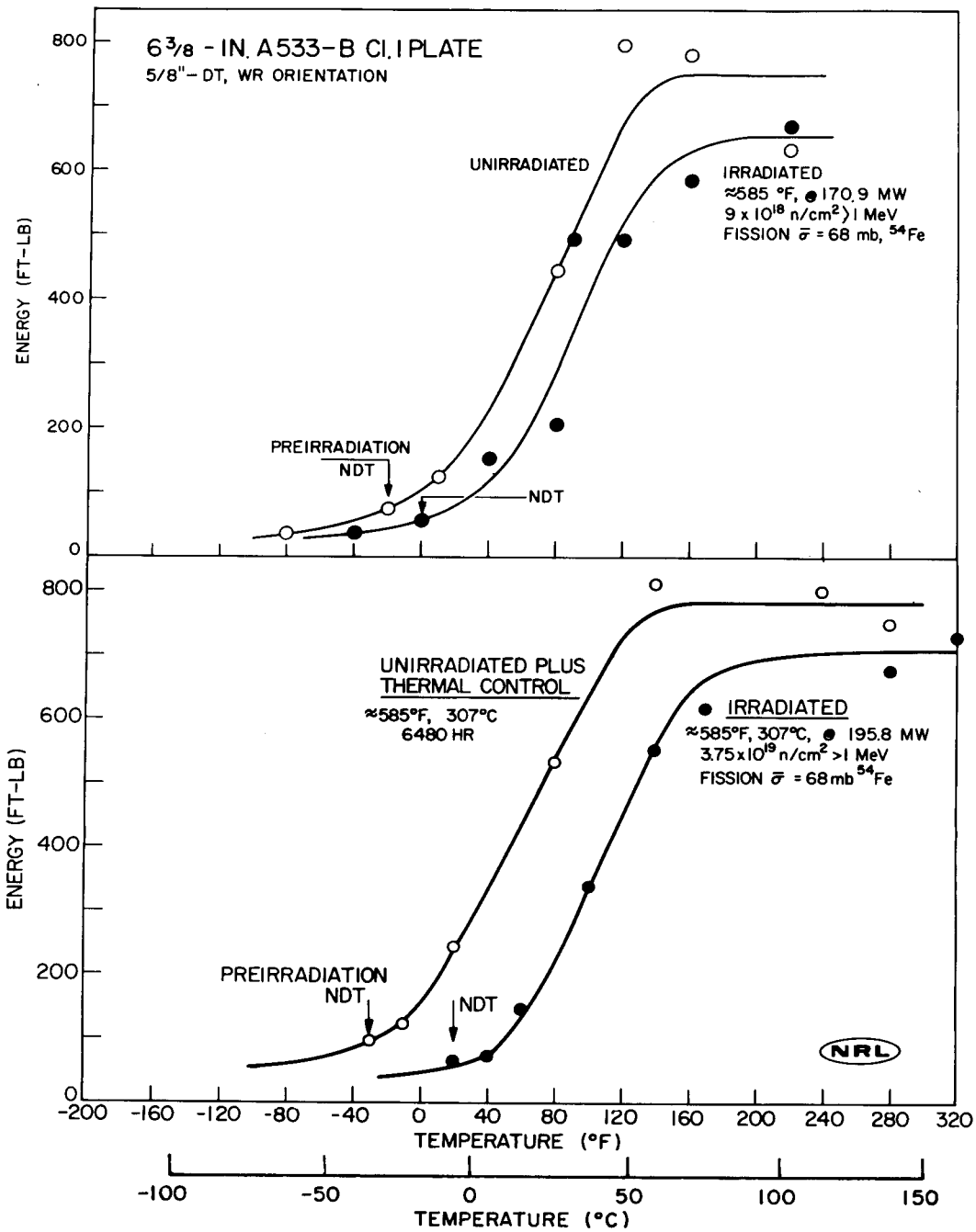

Fig. 2 - Comparison of 5/8-in. DT behavior before and after irradiation to two fluences. The irradiations were conducted in a commercial power reactor under realistic conditions of temperature and neutron spectrum. The NDT temperatures were determined from Drop Weight Tests.

The Fracture Transition Elastic (FTE)* temperature for thin sections, defined as NDT + 60°F in the FAD, must also be indexed within the transition temperature region exhibited by the DT test. Experience has shown that the FTE temperature usually lies within the temperature interval formed by the middle third of the 5/8-in. or 1-in. DT energy range for steels having a sufficiently high shelf toughness to exhibit gross plastic deformation. Considering the steel in Fig. 2, for example, the FTE is indexed by the low-temperature side of the middle-third energy for both the irradiated and unirradiated conditions. For steels of lower shelf toughness the FTE index can shift toward the high-temperature side of the middle-third energy. Steels such as A533-B which exhibit a sharp transition from brittle to ductile behavior define a temperature region corresponding to the middle-third energy that is narrow, usually less than 60°F, so that variations in indexing FTE from the DT curve are minimal.

CHARPY-V AND DYNAMIC TEAR TRANSITION TEMPERATURE COMPARISONS

Comparisons of the DT and C_v trends are required to determine the correspondence of these tests with respect to the definition of the temperature limits of the transition region, relative position of the NDT temperature, and the rate of increase in energy to a shelf level condition. In the case of irradiated steels it is also necessary to determine that the relationship between the C_v and DT trends remains fixed before and after irradiation. To achieve a meaningful comparison for irradiated steel, C_v, DT, and Drop Weight-NDT specimens must be irradiated to a common fluence and in an environment similar to that of a commercial power reactor with respect to neutron spectrum and temperature. Two such irradiations were conducted in accelerated surveillance locations of the Big Rock Point boiling water reactor at 585°F (307°C) using quarter-thickness (1/4 T) specimens from a 6-3/8-in.-thick plate of A533-B class 1 steel. The irradiations were carried to fluences of 9×10^{18} and 3.7×10^{19} n/cm^2 > 1 MeV. These values assumed a fission-spectrum distribution and a fission-spectrum-averaged cross section of 68 mb for the $^{54}Fe(n,p)^{54}Mn$ reaction. Procedures for determining fluences based on calculated neutron spectra are given elsewhere (8,9).

Pre- and postirradiation comparisons are presented for the 5/8-in. DT specimen in Fig. 2 and for the C_v specimens in Fig. 3. Also indicated in the figures are the pre- and postirradiation drop-weight NDT values; slight differences in plate location of the material for the two fluence levels of irradiation are believed responsible for the 10°F (6°C) preirradiation variations in NDT.

The 5/8-in. DT curves for the specimens in the WR (transverse or weak) orientation in Fig. 2 exhibit a sharp upsweep in energy from the toe of the curve, which is indexed by the NDT temperature in both the irradiated and unirradiated cases. The curve representing the unirradiated condition for the lower fluence irradiation was derived from specimens in the as-received condition; for the higher fluence irradiation, the as-received specimens were additionally heat treated at a time and temperature to match conditions for the irradiated specimens.

The C_v test results of RW (longitudinal or strong) orientation specimens from the irradiations at two fluence levels are shown in Fig. 3. The thermal control specimen results including those subjected to 800°F (427°C), 168-hr conditioning (simulating annealing treatments) "fit" the curves previously drawn from tests of as-received material. Thus, the neutron effects appear to be solely responsible for the transition region increases for all C_v results and also, by inference, for all DT results.

*The FTE denotes a temperature where yield stress levels are required to propagate flaws of large dimensions.

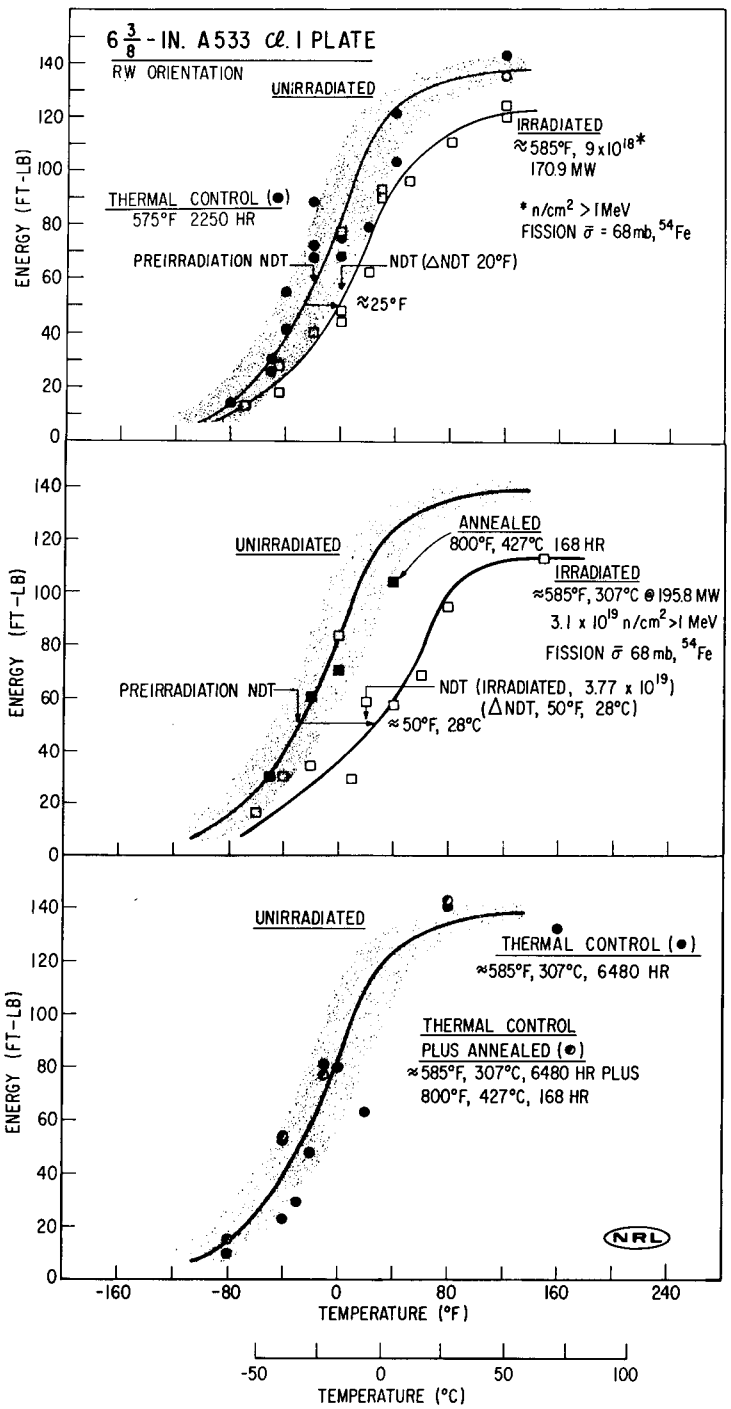

Fig. 3 - Comparison of pre- and postirradiation C_v trends from specimens irradiated simultaneously with the 5/8-in. DT specimens described in Fig. 2. Both types of specimens were from the same A533-B steel plate. The unirradiated curve is drawn through data from as-received plate which are not indicated in the figure. Results of unirradiated thermal control specimens are seen to fit the curve as drawn. The bottom curve (for clarity) illustrates the behavior of the thermal control specimens for the high fluence irradiation.

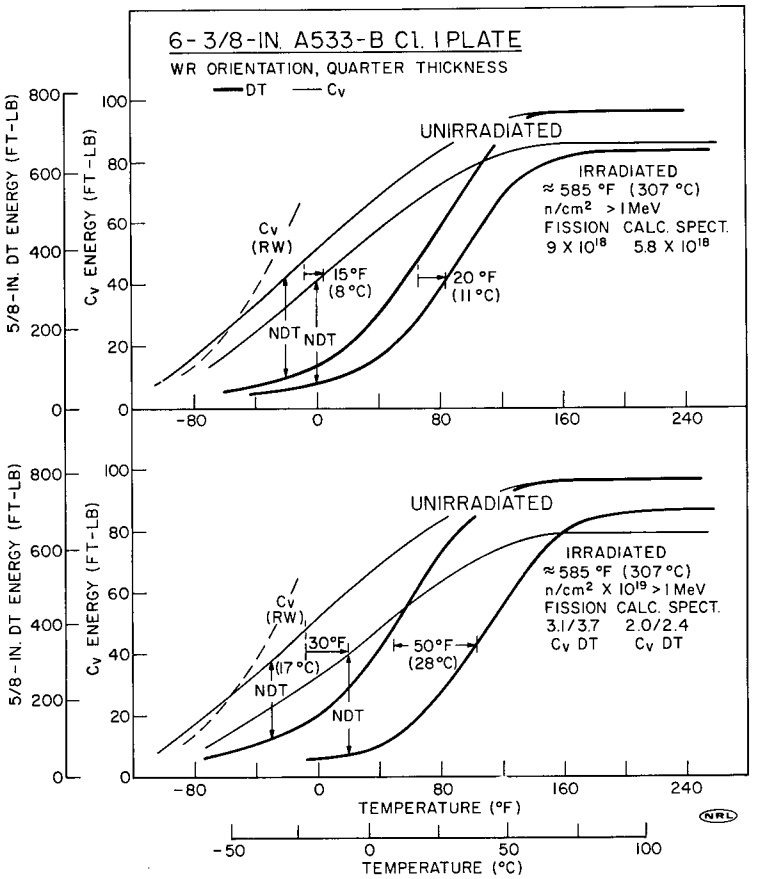

Fig. 4 - Comparison of the C_v and DT trends described in Figs. 2 and 3. The translation with irradiation of the temperature corresponding to the 50% shelf energy levels for both C_v and DT curves is seen to be in close agreement. This translation for the DT curve is a measure of the shift of the FTE temperature as described in the text.

It should be noted that the DT specimen results in Fig. 2 are of WR orientation while the C_v results are from RW orientation specimens. Intercomparisons of C_v and DT test behavior are best made with specimens of the same orientation. Therefore, data from the two Big Rock Point Reactor irradiations are compared on the basis of WR orientation behavior in Fig. 4. Here the DT curves are transposed directly from Fig. 2. The unirradiated C_v WR curve is drawn from existing data; the irradiated C_v WR curves are constructed from the irradiated C_v RW curves using the ratio of pre- and postirradiation C_v RW shelf values. This procedure is justified by previous research (10-12) that established constancy between WR and RW orientation trends in the transition temperature as well as the shelf level regions for identical irradiation conditions of the same steel plate.

The translation in the FTE temperature of the DT curves of both irradiations, as approximated by the 50% shelf energy level, compares very favorably with the NDT increase. The C_v curves demonstrate increases in the 50% shelf energy temperature similar to those of the DT curves. A more exact comparison between DT and C_v increases in the 50% shelf temperature for the higher fluence irradiation cannot be made because of the nominal difference in fluence levels of the C_v as compared with the DT and NDT

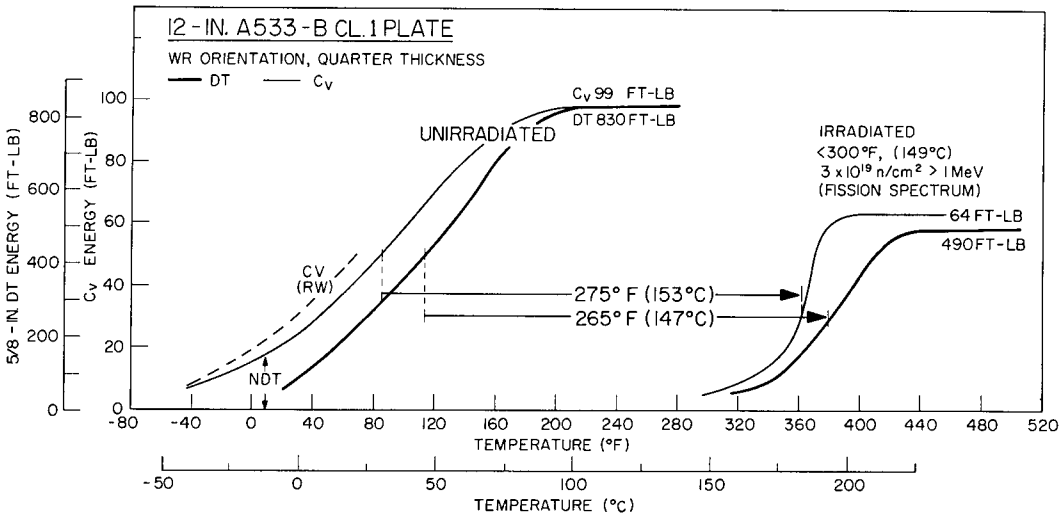

Fig. 5 - A comparison of the C_v and DT trends similar to that described in Fig. 4 but for a different plate irradiated at a low temperature, thereby resulting in a greater toughness degradation. Note that the correspondence of the C_v and DT 50% shelf temperatures is quite close.

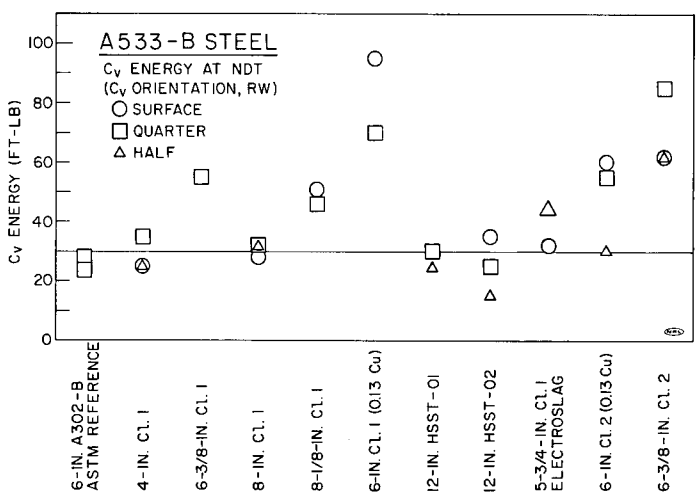

Fig. 6 - An illustration of the C_v energy corresponding to the Drop Weight-NDT temperature for numerous plates of A533-B and one weldment. The commonly used 30-ft-lb "fix" energy for the NDT temperature is seen to be unconservative and can result in errors of 40° F (22° C) or more in determinations at this temperature.

specimens (see Figs. 2 and 3 for exact differences). Note that the correspondence in shelf energy levels between C_v and DT is also in very good accord. A further example of the correspondence between the C_v and DT transition behavior is shown in Fig. 5. These data are for a low-temperature (< 300°F, 149°C) irradiation to 3×10^{19} n/cm^2 > 1 MeV of 12-in.-thick A533-B steel (13). As contrasted with the 585°F (307°C) irradiation, the low irradiation temperature results in much larger transition increases as measured by the DT and C_v 50% shelf energy levels; nevertheless, the C_v and DT increases are again seen to be in excellent correspondence.

The C_v WR energy levels corresponding to both the pre- and postirradiation NDT temperatures are seen to be identical in Fig. 4; this is the 40-ft-lb level, not the commonly assumed 30-ft-lb level. Inspection of Fig. 3 for RW orientation results shows the C_v energy level NDT "fix" to be between 50 and 60 ft-lb. This result agrees with earlier NRL results (10) showing consistently higher than 30-ft-lb "fix" levels for the NDT temperature in many representative plates and weldments of A533-B steel (Fig. 6). While the 30-ft-lb "fix" does index NDT for the two 12-in. HSST plates indicated in the figure and other plates, as seen in the literature, this behavior cannot be generalized in a conservative way. It is recommended that a more realistic C_v fix energy for A533-B steel should be 50 ft-lb for RW C_v data and 40 ft-lb for WR C_v data.

The preceding assessment of the C_v trends for A533-B steel shows them to be in good correspondence with the 5/8-in. DT trends for thin sections. The boundaries of the transition region for this steel, in both pre- and postirradiation conditions, can be acceptably indexed by the C_v test. The specific C_v energy values, however, attain a greater percentage of shelf energy than the DT curves at a given temperature above the NDT temperature. This nonconservatism associated with the C_v test is expected from past experience with this and other steels and is taken into account through the FAD analysis procedure which is based on DT behavior. It is concluded that the FAD procedure can apply equally well to irradiated material as well as unirradiated material subject to shelf level limitations described later. It is preferred to use the drop-weight test to define the NDT temperature, but the C_v test with the suggested revised "fix" energy gives an acceptable correlation.

TRANSITION TEMPERATURE CHARACTERISTICS OF THICK-SECTION A533-B STEEL

Earlier plane strain fracture toughness (K_{Ic}) tests conducted with A302-B, A533-B, and other transition temperature steels have shown that it is not possible to obtain valid static K_{Ic} values near NDT using small-size specimens (≈ 1 in. thick). With larger specimens capable of increased mechanical constraint, measurement capacity was extended for a small temperature increment into the transition region. On the basis of these observations it was argued that the brittle to ductile transition characteristics of these materials in very thick sections, representative of currently planned commercial reactor vessels, might be displaced well into the operating temperature region or eliminated entirely. If this was true, a serious concern for the fracture safety of these vessels could be caused. To characterize this problem, NRL conducted a research study of the transition temperature characteristics of thick A533-B steel plate using full-thickness DT specimens. A complementary investigation using similar material supplied by the AEC Heavy Section Steel Technology (HSST) Program was undertaken by Westinghouse Research Laboratories to determine how high in the transition temperature region valid K_{Ic} values could be obtained with specimens up to 12 in. thick (5).

NRL investigations centered on a 6-in. plate of A533-B class 2 steel and a 12-in. plate of A533-B class 1 steel (HSST plate 01). Both plates were representative of current steelmaking practices used in supplying the reactor vessel industry. The material properties, including C_v trends, are summarized in Ref. 14. Full-thickness DT tests were

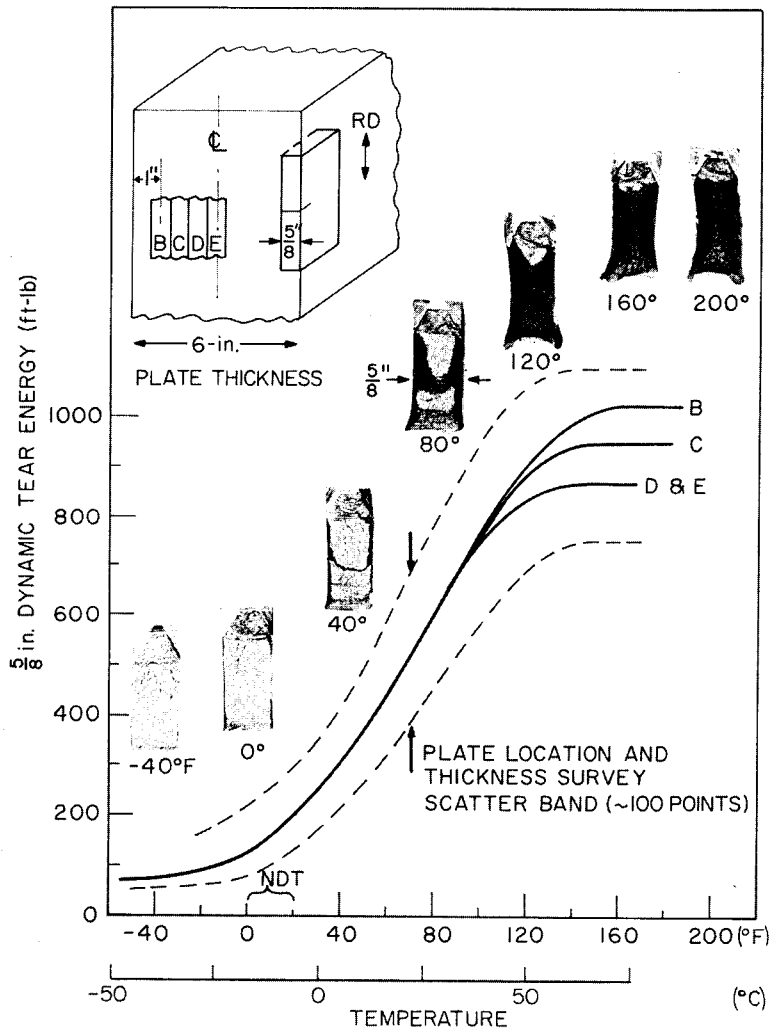

Fig. 7 - Variations in fracture toughness through the thickness of a 6-in. A533-B class 2 plate, determined by 5/8-in. DT specimens in the RW orientation. The fracture surfaces at selected temperatures are illustrated.

conducted for each plate in addition to 5/8-in., 1-in., and 3-in. DT tests to characterize the effects of increasing mechanical constraint with thickness. The fracture energy for all sizes of specimens for both plates exhibited an order of magnitude increase in the transition region. The fracture appearance likewise changed from cleavage near the toe of the DT curve to one of fully fibrous appearance and large lateral contraction, indicative of plastic behavior, near shelf temperatures.

Figure 7 illustrates a typical 5/8-in. DT energy trend along with photographs of selected fracture faces from specimens of the 6-in. plate. A comparison of fracture faces throughout the transition temperature region for various size specimens from the 6-in. plate is presented in Fig. 8. Similar trends were displayed by specimens from the 12-in. plate including the full-thickness tests. A complete fracture of a 12-in. specimen at the shelf temperature was not obtained, however, because the capacity of the drop weight

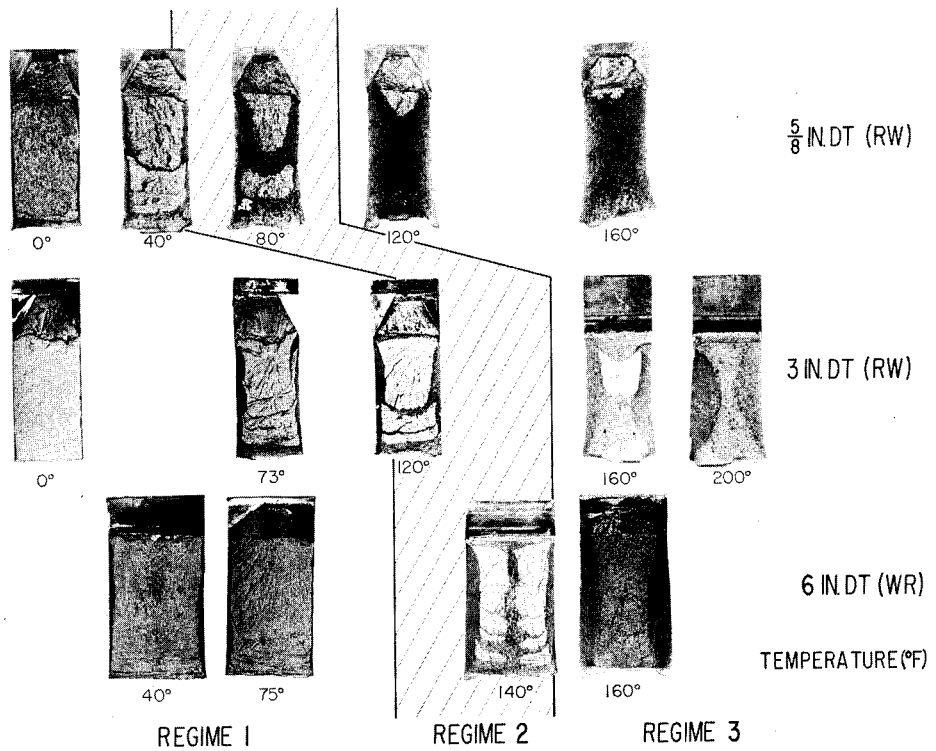

Fig. 8 - Composite photograph of the fracture surface of 5/8-, 3-, and 6-in. DT specimens as divided into three toughness regimes. Featureless, flat fractures of regime 1 are extended to higher temperatures by increased thickness. The arrest markings indicate a transition through regime 2. Fibrous fractures and lateral contraction features of regime 3 indicate completion of the transition.

machine was exhausted as a result of the rapid increase in fracture energy from 60,000 ft-lb near the NDT temperature to an estimated million foot-pounds at the shelf temperature. Figure 9 illustrates the 12-in. DT specimen which stalled the testing machine. This specimen exhibited a high degree of toughness as depicted by 7/16-in. lateral dimples on each side of the crack starter notch, the completely fibrous fracture appearance, and the partial tears at the base of the notch indicating the tendency to form a plastic hinge.

The specimens of similar fracture appearance in Fig. 8 have been grouped into three regimes. These regimes indicate a transition from flat fracture with small shear lips (regime 1) to fractures containing slight and then strong arrest markings (regime 2) and finally to fractures indicating large lateral contraction and rapidly increasing areas of fibrous tearing with increasing temperature (regime 3). The change in fracture appearance through regime 2 occurs within a narrow temperature range and the development of arrest markings in this regime is shifted to higher temperatures with increasing thickness, thereby indicating a thickness effect.

The DT energy trends from difference size specimens are compared for the 6-in. and 12-in. A533-B steel plates in Figs. 10 and 11, respectively. The DT energy is represented as energy/fracture area (E/A) in order to normalize small variations in the dimensions of the fractured area for a given size specimen. To compare the various sizes of

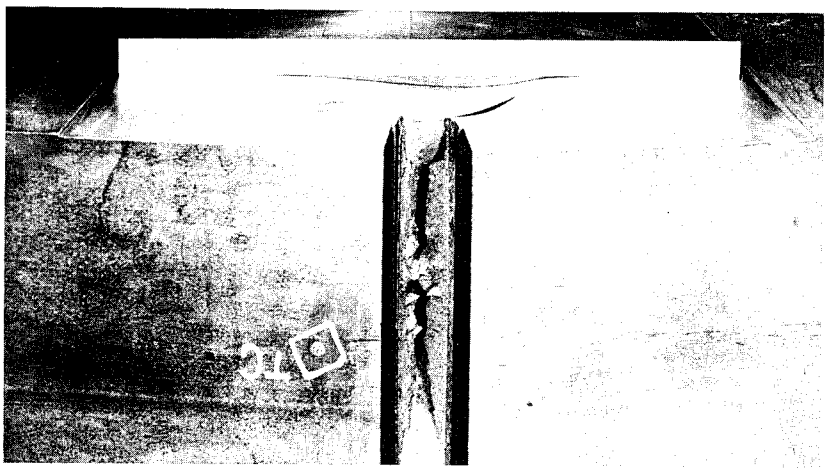

Fig. 9 - The 12-in. DT specimen which was partially fractured at 215°F (102°C). The scale indicates the large lateral dimple in the fracture path. Visible deformations under the scale show a deformed area over 1 ft wide.

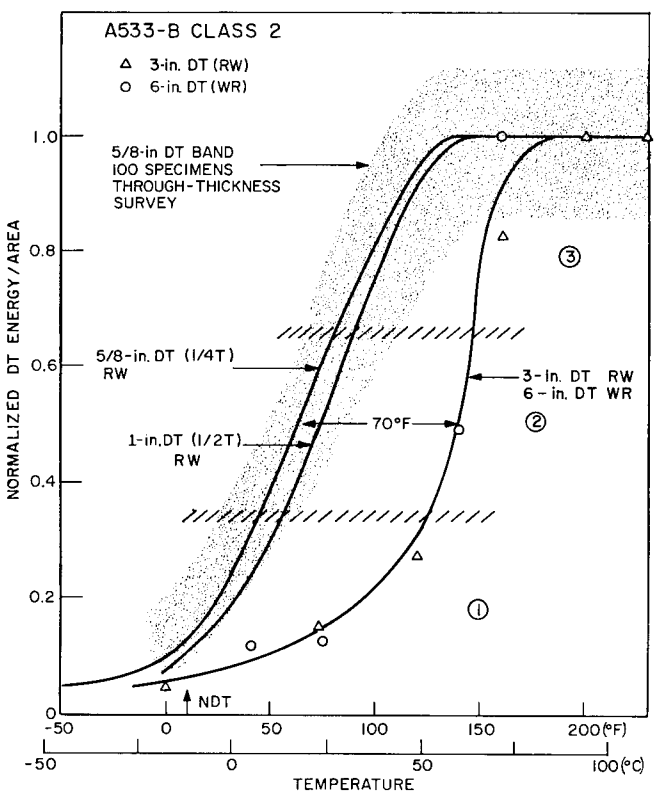

Fig. 10 - DT test curves for various thickness specimens from a 6-in. A533-B class 2 steel. The specimen energy trends are normalized on the basis of upper shelf energy/fractured area. The normalization procedure indicates a size effect by the shift in the FTE (taken as the DT energy midpoint) with thickness.

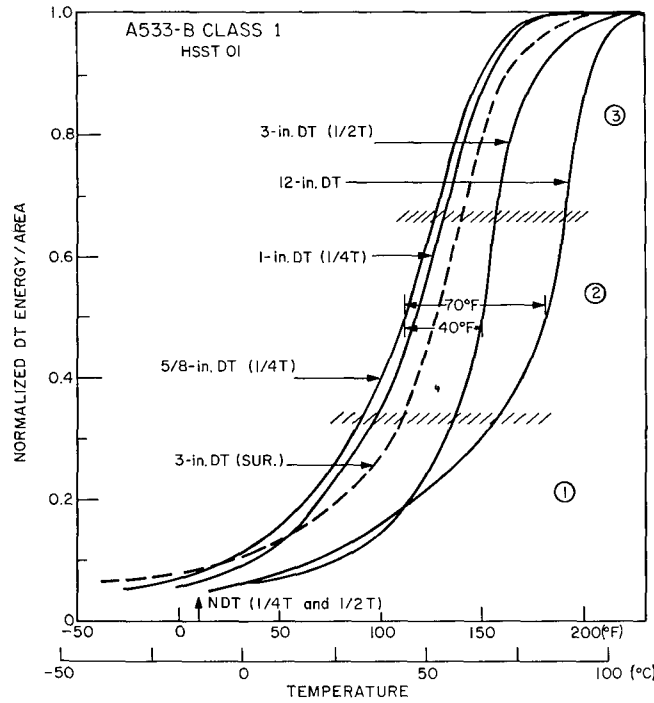

Fig. 11 - DT test curves for various thickness specimens in the RW orientation from a 12-in. A533-B class 1 steel plate (HSST 01). The specimen energy trends are normalized similar to those illustrated in Fig. 10. The behavior of the tough surface layer is indicated by the dashed 3-in. DT curve.

DT specimens the E/A values are restated as fractions of shelf energy for a given size specimen. Each of the resultant normalized curves is divided into thirds on the basis of shelf E/A, and it is found that this division results in the same temperature intervals for each regime as was determined from the comparison of the fracture faces (Fig. 8).

The fracture behavior of the different size specimens is judged to be similar in each temperature regime so defined when the shelf level behavior exhibits a high degree of plastic deformation as with the 6-in. and 12-in. DT specimens. In regime 3 there appear to be differences in the extent of plastic deformation between the different size specimens. These differences cannot presently be related to plastic load carrying capacity of a structure and therefore will not be discussed. Since plastic deformation is evident for all specimens at shelf temperature, the adoption of a common regime 3 nomenclature is possible. The regimes designate fracture behavior as follows: regime 1 — a region of relatively brittle behavior which can be analyzed with dynamic LEFM methods, regime 2 — a transition region which must contain the FTE requiring yield stress levels for fracture propagation, and regime 3 — a region near the shelf temperature in which gross plastic deformation is required to promote fracture.

The thickness effect is defined by the temperature displacement of the DT energy midpoint as an indication of the FTE. As seen in Figs. 10 and 11, the FTE defined in this manner increases with increasing section size but the effect appears to saturate with thickness. For example, material from the 12-in. plate shows a 40°F (22°C) increase in FTE from 5/8 in. to 3 in. and only an additional 30°F (17°C) increase from 3 in. to 12 in. The 6-in. plate shows no additional shift beyond 3 in. The thickness effect of 70°F (39°C) is taken to be indicative of that for thick-section A533-B, typical of current and planned reactor vessels.

Figures 10 and 11 show that the initial upsweep in energy absorption with thick sections near the NDT temperature is not as rapid as that for the 5/8-in. specimens in terms of percent of shelf level energy reached at a given temperature above the NDT temperature. Note that the 12-in. DT curve in Fig. 11 crosses the 3-in. DT curve from the 1/2 T location. This behavior is a result of the tough surface layer shown by the dashed 3-in. DT curve. Approximately 1 in. of plate surface material exhibits shelf level toughness near 0°F (-18°C), and this condition tends to override the effects of mechanical constraint for the initial upsweep in the 12-in. DT curve. The prolongation of the temperature interval of regime 1 due to the thick-section mechanical constraint indicates an extension of the temperature region analyzable with dynamic LEFM. With increasing temperature, however, the thick sections also exhibit a sharp increase in fracture toughness culminating in plastic deformation. This fact indicates the inability of thickness-induced constraint to overcome the sharp increase in micromode ductility with temperature.

A comparison of the 12-in. static K_{Ic} data generated by Westinghouse (15) and the 12-in. DT curve, both from HSST material, is presented in Fig. 12. The sharp upsweep of K_{Ic} with temperature corroborates the transition behavior shown by the large DT specimens. The use of the 12-in. K_{Ic} specimens extended the measurement capacity only to NDT + 40°F, where a ratio of K_{Ic}/σ_{ys} of 2.0 was determined. The infinity (∞) notation on the K_{Ic} curve signifies a projection to very high ratios and corresponding large increases in critical flaw sizes within a small temperature interval such that the use of LEFM is no longer justified. For specimens of less than the 12-in. thickness, the loss of mechanical constraint will necessarily result in the limit of linear elastic behavior occurring at lower temperatures. The question of there being a transitional behavior for thick-section A533-B steel plate similar to that exhibited by thin sections is therefore answered for steels of this toughness level.

Also indicated in Fig. 12 is the trend of the dynamic K_{Id} data from the literature (5). Until recently, data were available only to NDT - 30°F (17°C) using 1-in. specimens. An extrapolation of this data is continued to higher temperatures based on the 12-in. DT performance. Because of the rate sensitivity of A533-B steel, the K_{Id} values in the transition region are expected to be lower than the K_{Ic} values at given temperatures, but the sharp upsweep with temperature must complement the trend displayed by the DT curves. Indeed, recent data from Westinghouse tend to verify the K_{Id} projection made in the figure (16). The limit of valid K_{Id} data is not expected to exceed a temperature defined by the lower third of the 12-in. DT curve; that is, valid K_{Id} data cannot be obtained as high as the FTE temperature corrected for thickness. Tentative verification of this fact has been brought out in other research aspects of the HSST program (14).

The previous observations indicate that current reactor fracture-safe operating criteria for commercial plants must be revised to take cognizance of the elevation in FTE with thickness. (A revised FAD incorporating thick section behavior is presented in Ref. 5.) Based on the trends shown in Figs. 10, 11, and 12 it is suggested that the following modifications to the NDT + 60°F criterion will assure freedom from brittle fracture in terms of a large* flaw residing in stress fields up to yield levels. For sections over 3 in. thick an additional 70°F (39°C) should be added, and for thicknesses between 2 in. and 3 in. a temperature addition of 35°F (19°C) is suggested. The new temperature margins are felt to provide safety from brittle fracture for material containing a large flaw at yield stress levels even in the presence of dynamic loading whether due to a popin through locally embrittled material under static load or due to gross section dynamic loading. By virtue of the temperature displacement of the static and dynamic K_{Ic} curves in Fig. 12 additional conservatism is implied if dynamic loading as defined above is shown not to be possible.

*The flaw cannot be so large as to cause net section overload leading to plastic collapse or bulging in a vessel.

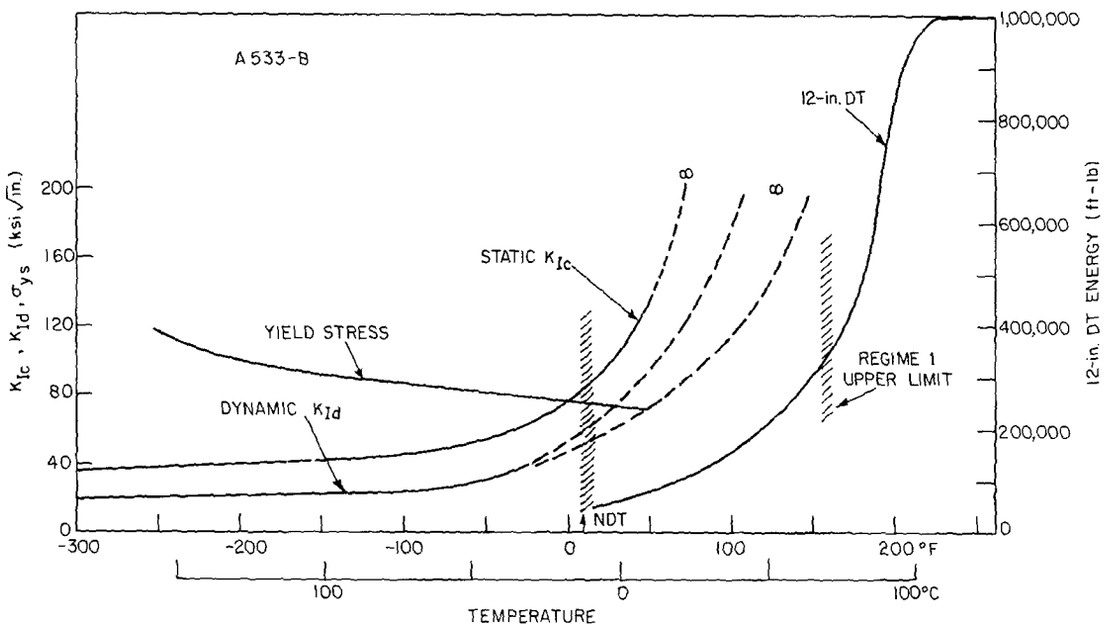

Fig. 12 - Comparison of thick-section DT tests with static (K_{Ic}) and dynamic (K_{Id}) data for A533-B steel. Large-section (12-in.-thick) K_{Ic} specimens did not *extend* the measurement capacity of static plane strain fracture toughness beyond NDT + 40°F (22°C). K_{Id} values are extrapolated to higher temperatures, but it is evident from the sharp rising region of the thick-section DT curve that K_{Id} specimens of large size would *not extend* the measurement capability beyond the limit defined by the DT tests.

A more definitive approach to this problem entails the determination of the dynamic K_{Id} at operating temperatures; if valid numbers can be obtained, then the critical flaw size can be defined for the stress level at the region in question. This determination is extremely difficult for irradiated material when thick sections are involved. If valid K_{Id} values cannot be obtained at the *operating* temperature because of high toughness, then additional quantitative methods of analysis (i.e., elastic-plastic approach) have not yet been developed to the point where it is feasible for the designer to use them.

SHELF LEVEL ANALYSIS

Thin Sections

The thickness-modified FAD analysis applied at the FTE temperature can provide safety from brittle fracture due to a large flaw at yield stress levels only if the shelf toughness is sufficiently high to require plastic overload for fracture propagation. If this toughness has been reduced by irradiation or is low to begin with, brittle fracture is possible at both the FTE and shelf temperatures. The critical flaw size-stress level conditions then may be treated with LEFM methods for sufficiently low shelf energies. The C_v and DT shelf energies cannot be related directly to critical flaw size and stress levels, and an interpretative procedure is required. Such a procedure has been developed

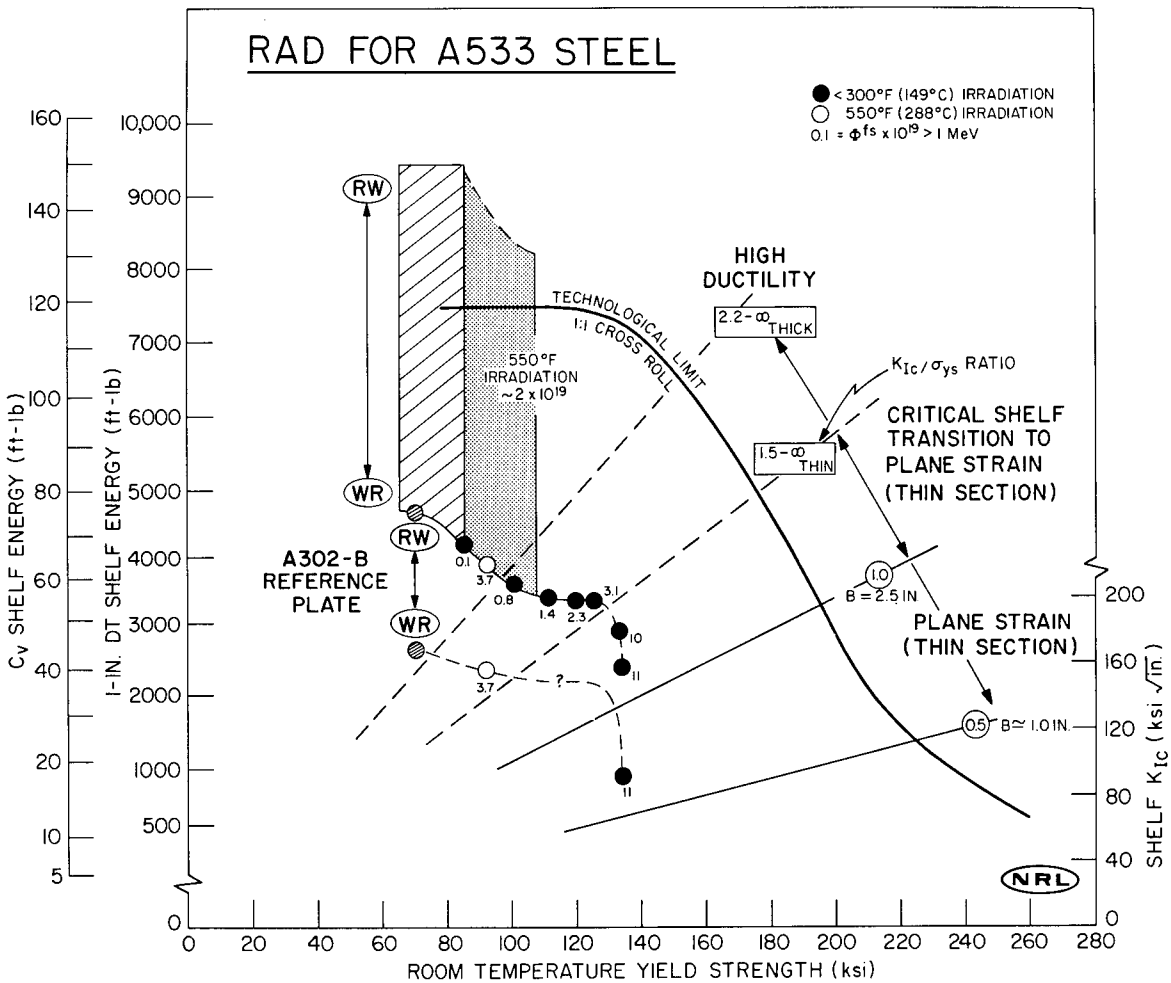

Fig. 13 - Ratio Analysis Diagram for A533-B steel illustrating pre- and postirradiation C_v shelf energy characteristics of A302-B steel and numerous A533 plates and weld metals

by Pellini in the form of the RAD (17). Interpretations of the RAD are first discussed in terms of thin sections (<3 in.); thick sections are discussed in the next section.

The RAD (Fig. 13) provides a means for critical assessments of the fracture resistance of steels and nonferrous alloys in the shelf level condition. The diagram presents a primary comparison of 1-in. DT shelf energy and yield strength. Since the DT test is not restricted to plane strain conditions, it can be used to define the full spectrum of metallurgical toughness from high ductility (high energy absorption, forced fracture) to plane strain conditions (low energy absorption, unstable fracture). A technological limit line is placed on the RAD indicating the DT performance of the best available steels at a given yield strength. This line is revised as better alloys become available. The 1-in. and 5/8-in. DT shelf energy values are interchangeable in the ratio of 8.0:1 as determined from a least-squares fit of data from over 25 different steels covering the entire energy scale (7).

The DT scale has been experimentally indexed to the K_{Ic} values obtained with higher-strength steels for which plane strain conditions are obtainable with specimens on the order

of 1 to 2 in. thick (17). The K_{Ic} and yield strength scales are placed on the diagram linearly and so permit a series of constant ratio lines of K_{Ic}/σ_{ys} to be drawn through the origin. The magnitude of the K_{Ic}/σ_{ys} ratio for plane strain conditions is a direct indication of the flaw size tolerance as can be readily verified from the K_{Ic} formulas in the literature. Increasing ratio numbers signify increasing fracture toughness, or alternatively, a larger flaw is required for instability at the same fraction of yield stress loading with increasing ratios. The RAD is zoned by three reference ratio lines: 0.5, 1.0, and $1.5-\infty_{thin}$. Material falling below the 0.5 ratio line is subject to fracture initiation from minute flaws (few tenths of an inch) which are difficult to detect. Materials indexed by increasing ratio lines above 0.5 exhibit a rapidly increasing tolerance for flaws since the critical flaw size is proportional to the square of the ratio. This increase in critical flaw sizes with increasing toughness continues to the point where plane strain conditions can no longer be maintained for a given thickness, and yield stress levels are eventually required for fracture propagation. This position on the RAD is denoted by the dashed thin-section infinity (∞) line.

To appreciate the significance of the ∞ line it must be realized that a minimum thickness is required to maintain the plane strain conditions necessary to measure a valid ratio. This thickness B is calculated from the relationship $B = 2.5(K_{Ic}/\sigma_{ys})^2$ currently required by the ASTM Committee E-24 on Fracture Toughness Testing. Thus, a thickness of 2.5 in. is necessary to measure a ratio of 1.0, and thicknesses of 5.6 in. and 10.0 in. are required to measure ratios of 1.5 and 2.0, respectively. For thin-section material, approximately 3 in. and less, positions of increasing toughness above the ratio 1.0 line signify that plane strain constraint is quickly lost because of extensive plastic deformation in the notch vicinity. Finally, yield stress levels and gross plastic deformation are required to propagate the fracture for DT toughnesses progressively above the infinity ratio. The position of the infinity line for thin-section materials has been verified by the plastic deformation exhibited by the DT specimens and also by the explosion tear test performance (17,18). Therefore, materials indexed in the region above the infinity ratio satisfy the condition of high shelf level toughness required by the FAD analysis to insure plastic loading for fracture propagation above the FTE temperature.

The K_{Ic} scale has been cross-indexed with the DT scale through experimental correlation using several higher-strength steels (>130-ksi yield strength) (17). It is felt that the correspondence continues to lower-strength steels, such as A533-B, which is being investigated. Qualitative verification of this conclusion is drawn from the fact that valid K_{Ic} values are not obtainable for shelf level A533-B steel; this steel is consistently indexed above the infinity line. With strain-rate-sensitive steels, like A533-B, there is some ambiguity as to which value of K_{Ic} (static or dynamic) is properly indexed by the RAD scale. It is felt, however, that the difference between static and dynamic behavior will be minimal at the shelf condition as compared with the transition region. At very high DT shelf toughness levels there is currently little definable difference between static and dynamic behavior. Therefore, an acceptable qualitative appraisal of fracture performance of A533-B-type steels can be obtained from the RAD. Additional testing with other methods is indicated for material indexed close to the infinity line, if exact relationships between flaw size and stress levels are required.

The C_v shelf energy has been indexed to the DT scale using the best-fit line through the data from 29 steels covering a wide range of toughnesses (17). An independent indexing of K_{Ic} to the C_v scale has confirmed the C_v scale position on the RAD (17). It is cautioned, however, that the C_v shelf energy does not always represent an accurate measure of the DT and K_{Ic} shelf toughness levels (4), and the RAD should be used with this test only when the C_v-DT correspondence has been verified. This verification was accomplished for numerous A533-B steel plates in both the irradiated and unirradiated conditions. The C_v-DT shelf correlation for these plates is presented in Fig. 14, and over 30 different toughness levels, as modified by irradiation, are indicated. Included in the comparison are data from high- and low-temperature irradiations resulting in wide

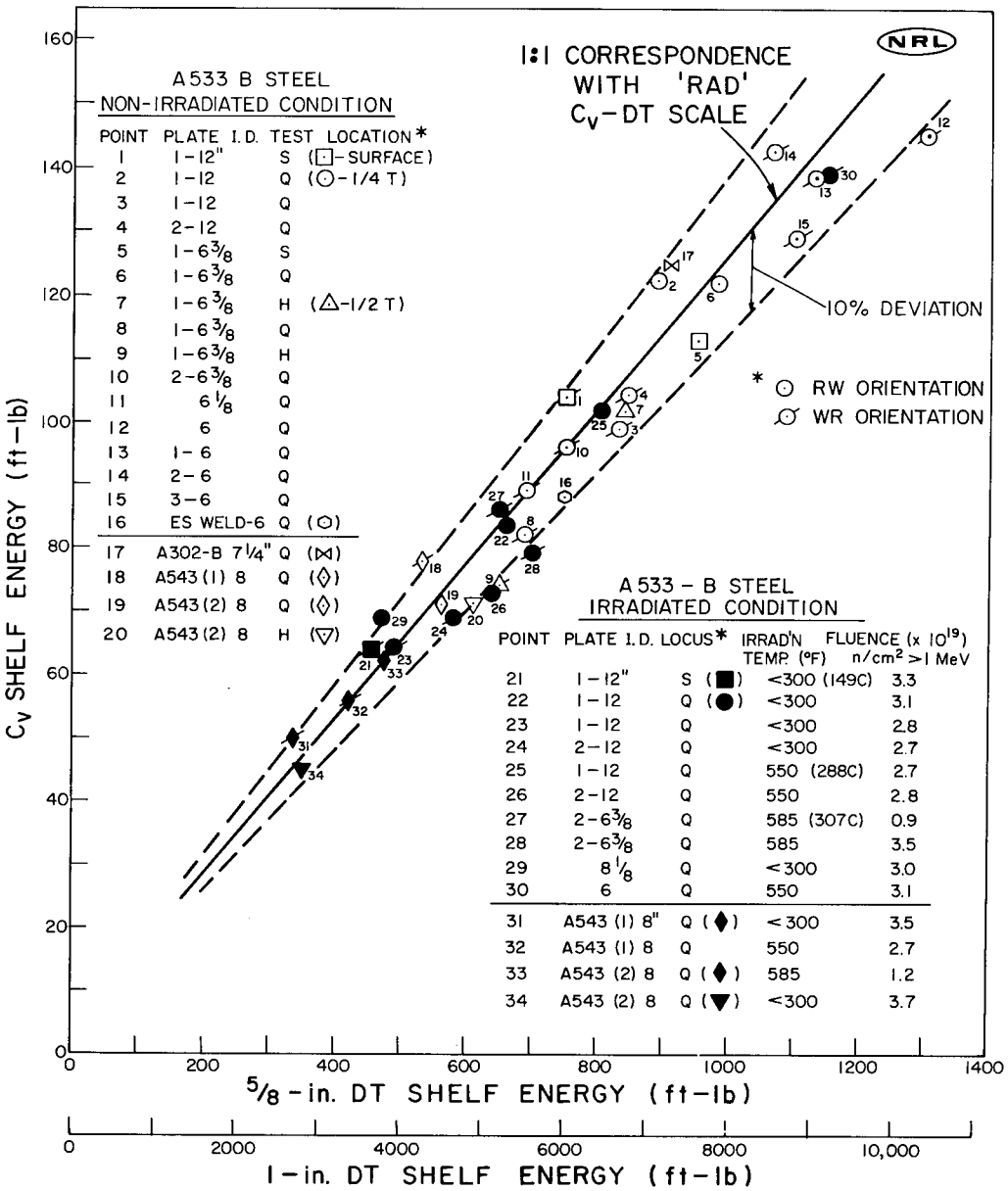

Fig. 14 - Pre- and postirradiation comparisons of C_v and DT shelf energies from numerous plates of A533-B. Comparisons are also illustrated from two plates of A543 steel, an A302-B plate, and an A533 electroslag weld.

variations in toughness and yield strength. The data are well represented by a band which deviates by ±10% from the predicted C_v-DT correlation using the RAD scales, which, incidently, were determined without data from A302-B or A533-B steels. Data developed on A543 steel plate, though not treated herein, are also indicated in support of the correlation. Some of the scatter in the irradiated data in Fig. 14 is attributable to the limited number of specimens provided by experimental irradiation subassemblies. On the basis of these comparisons, anticipated C_v shelf level* surveillance data from A533-B plates should be considered quite meaningful and may be used in conjunction with the RAD to predict fracture performance.

The C_v shelf behavior of numerous plates and weldments of A533 steel (grades B and C, classes 1 and 2) have been entered on the RAD in Fig. 13. Aggregate data are represented for the unirradiated (cross-hatched) and irradiated (shaded) conditions (11). The latter signify 550°F (288°C) irradiations to a fluence level of approximately 2×10^{19} > 1 MeV. The RW and WR properties generally reflecting plate cross-rolling history fall near the upper and lower regions of the bands, respectively. Based on A302-B tensile data for 550°F (288°C) irradiations (10), an average radiation-induced increase in room-temperature yield strength of 20 ksi was assumed for the various A533 plates and weld metals. The performance of the ASTM A302-B reference heat (6-in. plate) is also shown in the figure. The toughness degradation resulting from several different fluences <300°F (167°C) are shown as solid points. The two open points represent 550°F (288°C) irradiations of RW and WR specimens to a fluence of 3.7×10^{19} > 1 MeV.

Referring first to the performance of the A302-B steel, the data trend has several interesting features. Paralleling known trends in transition-temperature response, the RW C_v shelf values are shown to decrease rather rapidly during the initial 1×10^{19} n/cm^2 > 1 MeV of exposure at <300°F (167°C). The interval of 1 to 3×10^{19} n/cm^2 produces little additional change, although the yield strength is increased. Above this intermediate fluence plateau, a rapid reduction in shelf values is depicted with only small additional increases in yield strength. Data for the WR orientation, though limited, present similar trend indications. Significantly, the shelf energy of this steel when irradiated at 550°F (288°C) appears to follow the same damage path as described by data for the <300°F irradiation condition. Of course, the extent of embrittlement is less at the higher temperature and is believed due to beneficial thermal processes (vacancy annihilation) partially counteracting the detrimental irradiation processes (vacancy production).

The shaded areas of Fig. 13 are illustrative of the extent of variance in shelf values among A533 plate and weld metals in the unirradiated and 550°F (288°C) irradiation conditions. Although weak as well as strong plate orientations are well represented, all A533 values are shown to lie above the trend line (strong direction) for the A302-B reference heat and thus signify overall superior performance. This performance by the A533 data is considered a reflection of improved processing (cleaner heats) and the trend toward lower sulfur and phosphorus contents in the more recent A533 heats.

Using the RAD, the following assessment can be made with respect to the fracture performance of A533 steel in relatively thin sections. The 550°F (288°C) irradiation of plate and weld metals to fluences of 2×10^{19} > 1 MeV fall well above the ratio 1.5-∞ line and will require plastic overload for fracture propagation. Consequently, operation above the FTE temperature in the transition region should eliminate the possibility of brittle fracture up to yield stress levels. The ASTM reference heat indicates similar resistance to brittle fracture for the 550°F (288°C) irradiation to a fluence of 3.7×10^{19} n/cm^2 > 1 MeV.

*It is emphasized that positive indication must be given that the C_v values obtained are actually shelf values. This cannot be acceptably accomplished with just a few specimens, and it is recommended that the complete C_v curve be determined.

With increased fluences it is projected that the weak direction C_v shelf level for thin sections may be permitted to drop to 40 ft-lb and still insure that yield stress levels are required for fracture propagation. However, material displaying a shelf toughness of this low level and having a yield stress below 100 ksi, while lying above the ratio 1.5-∞ line, is not expected to exhibit high ductility, and failures are projected from flaws subjected to only limited amounts of plastic deformation.

In terms of 550°F (288°C) postirradiation shelf level performance, A533 weld metals on the basis of C_v indications appear comparable to A533 plate in requiring plastic overload for fracture propagation, at least for fluences to 2×10^{19} n/cm^2 > 1 MeV. At higher fluences, differences in individual shelf levels may become important, but on the whole, a performance "match" is indicated. Verification of matching radiation serviceability will, of course, depend on verification of a pre- and postirradiation C_v:DT shelf energy correlation for RAD entry such as that established for the plate in Fig. 14. Current correlation efforts involve both submerged arc and electroslag weldments fully representative of commercial practice. Initial results for a 6-1/4-in. electroslag weld deposit shown in Fig. 14 suggest that this correlation applies to A533 weld deposits of this type as well.

The general tendency of weld metals to develop lower pre- and postirradiation shelf values (11) compared to plate is seen to be further compounded by a generally higher susceptibility to radiation embrittlement at elevated temperature. Copper and phosphorus have been shown to be highly detrimental elements to radiation resistance at elevated temperature (19) and readily explain weld metal versus plate radiation resistance (10). Copper content, in particular, accounts for higher weld metal embrittlement tendencies as a copper clad is often applied to weld wire for corrosion resistance and better current-carrying capability. Notably, where copper content has been controlled at low levels, marked improvements in radiation embrittlement resistance have been achieved (19,20).

Thick Sections

The mechanical constraint associated with thick sections permits plane strain conditions to be retained to higher levels of toughness (e.g., higher C_v energies) than with thin sections. For example, it is possible to measure a valid ratio of K_{Ic}/σ_{ys} of 2.2 with a 12-in.-thick section according to ASTM thickness requirements. Note further that the ratio 2.2 line falls above the ratio ∞ line for thin sections and passes through the shaded band of elevated-temperature irradiations. From this fact one concludes that an irradiated 12-in. A533-B plate may fail in a brittle manner if the C_v shelf energy drops to 60 ft-lb (with an irradiated yield strength near 95 ksi).

The above conclusion must be tempered by the fact that a relatively large flaw is required for brittle fracture at this toughness level. For example, thick-section irradiated material is found at the vessel beltline where the stresses are relatively low, less than one-half yield stress. The depth of a 2:1 critical surface flaw, computed with K_{Ic} formulas available in the literature using a K_{Ic}/σ_{ys} ratio of 2.2, is equal to the section thickness (12 in.) at the one-half yield stress level. If the flaw is smaller than this critical value, plastic overload may be required for fracture. Second, the yield strength at operating temperatures is less than the room-temperature yield strength used to construct the RAD. This means that the shaded band in Fig. 13 would be shifted to the left by 5 to 10 ksi depending on the temperature of interest (11). Finally, properties through the plate thickness are not uniformly degraded by the radiation emanating from the reactor core due to self-shielding aspects as discussed elsewhere (8,21).

Unfortunately, no full-section fracture data exist for thick A533-B steel having a C_v shelf energy near 50 to 60 ft-lb on which to guide the placement of the ∞ line on the RAD for thicknesses on the order of a foot. From the 12-in. DT specimen shelf level performance previously described, which gave evidence of high plastic deformation in the

presence of a large flaw, it is known that an ∞ ratio line must lie significantly below the corresponding 115-ft-lb C_v and 70-ksi yield strength RAD index point for this specimen (i.e., ratio line of 5). This conclusion is borne out by the static and dynamic K_{Ic} data in Fig. 12, which indicate a ratio tending toward ∞ at the DT shelf temperature. There appears to be no concern for brittle fracture in using steel of this toughness level either unirradiated or irradiated to a fluence of approximately 2×10^{19} n/cm^2, as shown in Fig. 13, assuming a dropping C_v shelf trend with fluence as indicated for the A302-B reference plate. However, if the shelf level of 12-in., 80- to 95-ksi yield strength steel is on the order of 50 to 60 ft-lb in the orientation tested, it is possible that the thick-section toughness measurements will indicate a K_{Ic} shelf level near 200 ksi $\sqrt{\text{in.}}$ This in turn will help establish the position of the ratio ∞ line for thick sections.

Additional research must be undertaken to better resolve this area of uncertainty. As a first approximation, plates should be obtained from specially prepared melts of A533-B having a low cross-rolling ratio and made with a low level of cleanliness to obtain C_v shelf energies in the range of 50 to 60 ft-lb (80- to 95-ksi yield strengths). This artificial lowering of the C_v shelf will not exactly duplicate the damage mechanisms resulting from irradiation, but nevertheless it is felt to be a logical first step in view of the difficulties in irradiating and testing sections on the order of a foot thick. This approach, of course, assumes that a K_{Ic} shelf will not be obtained for the yield strength range of interest with smaller specimens featuring less constraint that can be conveniently irradiated. With an evaluation of the low shelf energy plates, the toughness associated with C_v shelf data from reactor surveillance irradiations could be put into perspective both with respect to fracture at shelf temperatures and with respect to the validity of the application of the thick-section FTE temperature for operation in the transition temperature regime.

SUMMARY

This report has presented a reappraisal of the fracture-safe operating criteria in general use for commercial water-cooled nuclear pressure vessels. These criteria were founded, in part, in the Fracture Analysis Diagram interpretative procedure for steels of relatively thin sections.

The FAD analysis was evolved from service failure correlations of unirradiated steel and shows that large flaws loaded up to yield stress levels will not propagate above the FTE temperature defined as NDT + 60°F. The validity of this diagram rests in the commonly observed brittle to ductile transition for low-alloy steels, which evolves within a limited temperature interval above the NDT temperature. A C_v "fix" energy is often used to derive an approximate Drop Weight-NDT temperature for these steels.

Progressive radiation damage to a reactor vessel is assessed from shifts in the NDT temperature as determined from C_v surveillance specimens irradiated with the vessels. However, implications from fracture mechanics tests of thin sections applied to project the trends of thick sections suggested that the increased mechanical constraint associated with the latter may severely depress or eliminate the brittle to ductile transition. Increased emphasis was also placed on the fact that a low C_v shelf energy, resulting from irradiation, could effectively eliminate the sharp transition to ductile behavior. Both of these possibilities gave stimulus to this reappraisal of the fracture prevention criteria and the applicability of toughness determinations from the C_v test to irradiated thick-section vessels.

The DT test procedure is considered to provide a definitive approach to fracture prevention and overcomes limitations of the C_v test which have proven the latter to be misleading in certain applications. The C_v and DT test performances were compared for A533-B steels typical of commercial reactor vessel construction, and the conclusions reached in this report apply primarily to this steel. The results of comparisons of

unirradiated plate material as well as comparisons of material irradiated to simulate the vessel wall of a commercial power reactor show that the C_v specimen can generally characterize the temperature limits of the transition region as defined by the DT test and can also accurately index changes in toughness with irradiation. However, specific C_v energy levels within the transition region do not necessarily provide a proper indication of fracture resistance in view of the fact that this energy can be a greater percentage of shelf energy than the DT energy at a given temperature above the NDT temperature. The C_v 30-ft-lb energy commonly used to index the Drop Weight-NDT does not yield consistently conservative results for A533-B steel, and in the absence of measured NDT values, it is recommended that values of 40 and 50 ft-lb be used with WR and RW C_v specimens, respectively.

The DT investigations of the transition behavior of thick-section (12-in.) A533-B plate indicated that the mechanical constraint associated with these thicknesses can broaden the temperature region of low toughness near the NDT temperature as compared to that exhibited by thin sections. This constraint, however, cannot suppress the eventual transition to high toughness requiring plastic deformation to propagate large flaws for the quality of steel investigated. These findings are corroborated by thick-section fracture mechanics tests conducted by the Westinghouse Research Laboratories using similar material. It was concluded from the DT investigation that the FTE temperature for thick sections is elevated by approximately 70°F (39°C) over that associated with very thin sections, less than 1 in. thick. Existing criteria for fracture safety based on operations above the FTE temperature, defined as NDT + 60°F, should be adjusted to reflect this thickness effect.

The significance of the C_v shelf energy in terms of a critical flaw size-stress level relation has been assessed by means of the Ratio Analysis Diagram, which has cross-indexed the DT and K_{Ic} toughness levels for different materials. An indication of toughness is determined from the position of one of the above two quantities with respect to a family of constant K_{Ic}/σ_{ys} ratio lines. The limited constraint associated with thin sections permits the placement of a thin-section ratio ∞ line on the RAD, determined by means of DT specimen behavior, to indicate toughness levels requiring in excess of yield stress loadings for fracture propagation. The DT test indexing provides a means to traverse the full spectrum of toughness from brittle to ductile behavior, including the regime of high toughness associated with plastic deformation for which K_{Ic} values are not defined. For A533 steel the C_v shelf energy has now been successfully indexed to the DT shelf energy for a wide range of toughnesses. Thus, direct access to the RAD has been gained for reactor vessel C_v surveillance data. Using C_v results, the irradiated and unirradiated performances of many typical heats of A533-B steel were entered on the RAD for comparison purposes. These representative data suggest that a sufficiently high C_v shelf toughness, for thin sections, is maintained even after moderate irradiation to assure plastic deformation requirements for fracture propagation and continued applicability of the FAD analysis.

The increased constraint associated with very thick sections ($\approx$12 in.) permits higher K_{Ic}/σ_{ys} ratios to be determined under plane strain conditions and necessarily elevates the position of the ∞ ratio line determined for thin sections. Insufficient fracture data exist from thick sections having low shelf energies to properly index this ∞ line; however, a conservative upper boundary has been defined from an investigation of thick A533-B plate of high shelf toughness. It is estimated from the RAD that thick sections of unirradiated A533-B steel having a yield strength of 70 ksi could exhibit a brittle behavior at C_v shelf energies near 40 ft-lb. Likewise, irradiated steel having yield strengths on the order of 80- to 95-ksi and 50- to 60-ft-lb C_v shelf energies may exhibit brittle fracture in the presence of an appropriate flaw. It is suggested that specially prepared melts of A533-B having the above properties be procured and tested in order to obtain a better understanding of the fracture characteristics of thick-section, low-shelf-energy irradiated steel and thereby provide a more exact means for the interpretation of C_v surveillance data.

REFERENCES

1. "Method for Conducting Drop-Weight Test to Determine Nil-Ductility Transition Temperature for Ferritic Steels," 1968 Book of ASTM Standards, Part 31, Philadelphia:American Society for Testing and Materials, pp. 673-691, May 1968

2. Pellini, W.S., and Puzak, P.P., "Fracture Analysis Diagram Procedures for the Fracture-Safe Engineering Design of Steel Structures," NRL Report 5920, Mar. 15, 1963; also Welding Res. Council Bull. 88, May 1963

3. Pellini, W.S., Steele, L.E., and Hawthorne, J.R., "Analysis of Engineering and Basic Research Aspects of Neutron Embrittlement of Steels," Welding J. 41 (No. 10):455-S-469-S (1962)

4. Lange, E.A., and Loss, F.J., "Dynamic Tear Energy — A Practical Performance Criterion for Fracture Resistance," ASTM Special Technical Publication 466, Impact Testing of Metals, Mar. 1970

5. Loss, F.J., and Pellini, W.S., "Coupling of Fracture Mechanics and Transition Temperature Approaches to Fracture-Safe Design," NRL Report 6913, Apr. 14, 1969; Practical Fracture Mechanics for Structural Steel, London:Chapman and Hall, pp. J1-J35, Aug. 1969

6. Lange, E.A., Puzak, P.P., and Cooley, L.A., "Standard Method for the 5/8-Inch Dynamic Tear Test," NRL Report 7159, in publication

7. Puzak, P.P., and Lange, E.A., "Standard Method for the 1-Inch Dynamic Tear Test," NRL Report 6851, Feb. 1969

8. Serpan, C.Z., Jr., and Hawthorne, J.R., "Yankee Reactor Pressure Vessel Surveillance: Notch Ductility Performance of Vessel Steel and Maximum Service Fluence Determined from Exposure During Cores II, III, and IV," Trans. ASME (J. Basic Eng. 89 (Series D, No. 4):897-910 (1967)

9. Potapovs, U., Hawthorne, J.R., and Serpan, C.Z., Jr., "Notch Ductility Properties of SM-1A Reactor Pressure Vessel Following the In-Place Annealing Operation," NRL Report 6721, May 1968; also Nucl. Appl. 5 (No. 6):389-409 (1968)

10. Hawthorne, J.R., and Potapovs, U., "Initial Assessments of Notch Ductility Behavior of A533 Pressure Vessel Steel With Neutron Irradiation," NRL Report 6772, Nov. 1968; also ASTM STP 457, "Effects of Radiation Structural Metals," pp. 113-134, 1969

11. Hawthorne, J.R., "Trends in Charpy-V Shelf Energy Degradation and Yield Strength Increase of Neutron-Embrittled Pressure Vessel Steels," NRL Report 7011, Dec. 1969; also Nucl. Eng. Design 11 (No. 3):427-446 (1970)

12. Serpan, C.Z., Jr., "Neutron Radiation Embrittlement of LaCrosse Reactor Pressure Vessel Steel and Weldment: Properties and Directionality Considerations," Nucl. Eng. Design 8:95-107 (1968)

13. Hawthorne, J.R., "Postirradiation Charpy-V and Dynamic Tear Shelf Level Performance of 12-in. Thick A533-B Plates and Weld Metal," NRL Memorandum Report 2114, Apr. 1970

14. Loss, F.J., "Dynamic Tear Test Investigations of the Fracture Toughness of Thick-Section Steel," NRL Report 7056, May 1970

15. Wessel, E.T., "Linear Elastic Fracture Mechanics for Thick-Walled, Welded Steel Pressure Vessels: Material Property Considerations," Practical Fracture Mechanics for Structural Steel, London:Chapman and Hall, pp. H1-H44, Aug. 1969

16. Shabbits, W.,"Rate Effects Studies on A533, Grade B, Class 1 Steel," presented at Heavy Section Steel Technology Program 4th Annual Information Meeting, Mar. 31-Apr. 1, 1970, Oak Ridge, Tennessee

17. Pellini, W.S., "Advances in Fracture Toughness Characterization Procedures and in Quantitative Interpretations to Fracture-Safe Design for Structural Steels," NRL Report 6713, Apr. 3, 1968; also Welding Res. Council Bull. 130 (May 1968)

18. Pellini, W.S., et al., "Review of Concepts and Status of Procedures for Fracture-Safe Design of Complex Welded Structures Involving Metals of Low to Ultra-High Strength Levels," NRL Report 6300, Jun. 1965

19. Potapovs, U., and Hawthorne, J.R., "The Effect of Residual Elements on 550°F Irradiation Response of Selected Pressure Vessel Steels and Weldments," NRL Report 6803, Nov. 1968; also Nucl. Appl. 6 (No. 1):27-46 (1969)

20. Hawthorne, J.R., "Demonstration of Improved Radiation Embrittlement Resistance of A533-B Steel Through Control of Selected Residual Elements," NRL Report 7121, Jan. 1970

21. Serpan, C.Z., Jr., and Hawthorne, J.R., "Through-Thickness Notch Ductility and Tension Properties as a Function of Neutron Exposure to a Simulated Pressure Vessel Wall of A302-B Steel," NRL Report 6575, June 1967; also Nucl. Eng. Design 6 (No. 1):78-88 (1967)